Progressive Kidney Degeneration in Mice Lacking Tensin

Su Hao Lo,* Qian-Chun Yu,* Linda Degenstein,* Lan Bo Chen,‡ and Elaine Fuchs*

*Howard Hughes Medical Institute, Department of Molecular Genetics and Cell Biology, The University of Chicago, Chicago, Illinois 60637; and ‡Dana Farber Cancer Institute, Harvard Medical School, Boston, Massachusetts 02115

Abstract. Tensin is a focal adhesion phosphoprotein that binds to F-actin and contains a functional Src homology 2 domain. To explore the biological functions of tensin, we cloned the mouse tensin gene, determined its program of expression, and used gene targeting to generate mice lacking tensin. Even though tensin is expressed in many different tissues during embryogenesis, tensin null mice developed normally and appeared healthy postnatally for at least several months. Over time, −/− mice became frail because of abnormalities in their kidneys, an organ that expresses high levels of tensin. Mice with overt signs of weakness exhibited signs of renal failure and possessed multiple large cysts in the proximal kidney tubules, but even in tensin null mice with normal blood analysis, cysts were prevalent. Ultrastructurally, noncystic areas showed typical cell–matrix junctions that readily labeled with antibodies against other focal adhesion molecules. In abnormal regions, cell–matrix junctions were disrupted and tubule cells lacked polarity. Taken together, our data imply that, in the kidney, loss of tensin leads to a weakening, rather than a severing, of focal adhesion. All other tissues appeared normal, suggesting that, in most cases, tensin's diverse functions are redundant and may be compensated for by other focal adhesion proteins.

FOCAL adhesions are specialized cell–substratum junctions that are nearly ubiquitous among cells that attach to an extracellular matrix. At the core of the focal adhesion is a cluster of activated integrin heterodimers, which are transmembrane signaling proteins that attach cells to their ligands, i.e., extracellular matrix (ECM)[1] (Hynes, 1992). β1 integrin, coupled with one of its many α partners, is thought to play a central role in focal adhesion formation. Inside the cell, activated integrins anchor the actin cytoskeleton to the plasma membrane (Burridge et al., 1988; Jockusch et al., 1995). Focal adhesions are thought to participate in many diverse biological processes including cell attachment, migration, polarization, growth, death, differentiation, embryogenesis, and tissue development (Burridge et al., 1988; Hynes, 1992; Jockusch et al., 1995; Schwartz et al., 1995).

Focal adhesions were first identified in tissue-culture cells, as sites of contact between a cell and its underlying substrate (Abercrombie et al., 1971). Terminating at these sites are bundles of actin microfilaments, referred to as stress fibers. At the interface between activated β1 integrins and stress fibers are a number of structural and signaling proteins, including talin, vinculin, α-actinin, paxillin, Src, protein kinase C, focal adhesion kinase, zyxin, p130cas, and tensin (Burridge et al., 1988; Jockusch et al., 1995). These proteins form a complex around the cytoplasmic domains of the integrin subunits, suggesting a dual role for this complex in cytoskeletal architecture and in signal transduction. In vitro binding assays have suggested that talin and α-actinin may associate directly with β1 integrin (Horwitz et al., 1986; Otey et al., 1990). Kinetic studies have suggested that localization of tensin and focal adhesion kinase to sites of integrin clustering are also early events in the formation of focal adhesions (Miyamoto et al., 1995).

Of the myriad of focal adhesion proteins, tensin is particularly interesting because it has the ability to bind to actin microfilaments at multiple sites, enabling tensin both to cap the growing (barbed) ends of actin filaments and to cross-link actin filaments (Lo et al., 1994*a*; Chuang et al., 1995). In addition, tensin is phosphorylated on tyrosine, threonine, and serine residues (Lo et al., 1994*c*). The phosphorylation of tensin's tyrosine residues occurs upon integrin activation by ECM (Bockholt and Burridge, 1993), as well as by transformation of cells with oncogenes such as v-src, BCR/ABL (Davis et al., 1991; Salgia et al., 1995). Tensin also has an Src homology 2 (SH2) domain, which makes it a candidate to bind to other proteins which themselves are tyrosine phosphorylated. One association mediated through tensin's SH2 domain occurs with PI3 kinase: upon PDGF stimulation, ~1% of the total PI3 kinase activity is present in tensin immunoprecipitates (Auger et al.,

Please address all correspondence to Elaine Fuchs, Howard Hughes Medical Institute, Department of Molecular Genetics and Cell Biology, The University of Chicago, 5841 S. Maryland Avenue, Room N314, Chicago, IL 60637. Tel.: (773) 702-1347. Fax: (773) 702-0141.

1. *Abbreviations used in this paper*: ECM, extracellular matrix; ES, embryonic stem; GST, glutathione-*S*-transferase; SH2, Src homology 2.

1996). Another interaction likely to be mediated by tensin's SH2 domain is the focal adhesion molecule p130cas: in this case, tensin-conjugated beads associate specifically with the p130cas present in lysates isolated from Rous sarcoma virus–transformed fibroblasts (Lo et al., 1994*c*). The diversity of interactions between tensin and other cellular proteins, coupled with the activation of these associations by growth factors or integrins, suggests that tensin is not only a cytoskeletal-membrane linker protein, but also a signal transducer (Lo et al., 1994*c*).

To understand more about tensin's possible roles in tissues in vivo, we have isolated and characterized a mouse tensin cDNA and gene, and we have analyzed the expression of tensin during embryogenesis and postnatal development. To assess the extent to which tensin is functionally important in these tissues and to elucidate the significance of tensin's many associations, we have used gene targeting in embryonic stem cells to generate tensin null mice. Analysis of the tensin null mice and the expression patterns of tensin during embryonic and postnatal development reveals a number of surprising and intriguing results. Specifically, we find that (*a*) tensin is not required for mouse embryogenesis, or for the postnatal functioning of many tissues that normally express tensin; and (*b*) tensin null mice develop kidneys that harbor multiple tubular cysts and progressive dilatation of the renal pelvis often without leading to mortality.

Materials and Methods

Isolation and Characterization of Mouse cDNA and Genomic Clones for Tensin

An 890-bp mouse tensin cDNA fragment was generated by PCR using primers 5′-TACATGCACTACAGCAA-3′ and 5′-GTGGAGTTGCCCG AGTC-3′ and cDNAs from a mouse lung cDNA library (Clontech, Palo Alto, CA). Primers were based on the published chicken cDNA sequence (Lo et al., 1994*b*). The identity of the tensin cDNA fragment was confirmed by DNA sequencing, and the cDNA was then radiolabeled and used to screen the same lung cDNA library, as well as a 129SV mouse genomic library (a gift from P. Soriano, University of Washington). Six cDNA clones and one genomic clone were identified and subsequently purified. Clone L52 contained a 1.2-kb cDNA insert, which was subsequently used as a probe for Northern blot analysis and for in situ hybridization. The genomic clone was subjected to restriction map analysis and used for making the targeting vector.

Generation of Tensin −/− Mice

The targeting vector was electroporated into embryonic stem (ES) cells (R1 strain from Andreas Nagy and Janet Rossant, University of Toronto, Canada), treated at 300 V and 500 μF in a GenePulser (Bio Rad Laboratories, Hercules, CA). Cells were then plated on eight 10-cm plates containing G418-resistant mouse embryonic fibroblast feeder cells. 24 h later, selection was initiated using 250 μg/ml active G418 and 2 μM gancyclovir. After 10 d of selection, double-resistant colonies were picked and transferred in duplicate onto fresh feeder cells for expansion of the ES colonies. Cells from one plate of each clone were trypsinized and stored in 10% DMSO at −80°C.

Cells from the other plate were incubated for 12 h at 55°C in the presence of DNA extraction buffer (20 mM NaCl, 1% SDS, 1 mM EDTA, 0.2 mg/ml proteinase K, 50 mM Tris-HCl, pH 8). These cell solutions were then phenol-extracted and precipitated with 20 mM sodium acetate in 95% ethanol. DNAs were assayed by Southern blot analysis.

ES cells carrying the mutant allele were injected into the inner cell mass of C57BL6 blastocysts. Chimeric mice with a high (>65%) contribution to coat color from 129SV were bred for germline transmission. For genotyping, genomic DNAs isolated from ES cells or mouse tails were digested with EcoRI for 5′ probe or BamHI for 3′ and Neo probes.

Immunoblot, Northern, and Southern Analyses and In Situ Hybridizations

Immunoblot, Northern, and Southern analyses were performed as described (Guo et al., 1995). In situ hybridization of paraffin sections was performed using digoxigenin-labeled antisense riboprobes as described (Chiang and Flanagan, 1996).

Generation of Tensin Antibodies

Glutathione-*S*-transferase (GST)–tensin fusion proteins engineered to contain the L52 tensin fragment, encoding amino acid residues 338–748 (corresponding to the chick tensin coding sequence), were purified and injected to rabbits for antisera as described (Lo et al., 1994*b*). The p130cas antibodies were raised against GST fusion proteins containing amino acid residues 487–968 of rat p130cas (Sakai et al., 1994). Antisera were purified by passage through GST Sepharose columns (Sigma Chemical Co., St. Louis, MO).

Ultrastructural Analysis

For regular EM, tissues were fixed at room temperature for at least 1 h with 2.5% glutaraldehyde and 4% paraformaldehyde in 0.2 M sodium cacodylate buffer (pH 7.4). Samples were trimmed and washed three times with the same buffer, and then postfixed with 1% aqueous osmium tetroxide for 1 h at room temperature. These samples were further washed with sodium cacodylate buffer, followed by maleate buffer (pH 5.1), and stained en bloc with 1% uranyl acetate for 1 h at room temperature. The samples were then washed several times with maleate buffer, dehydrated with cold ascending grades of ethanol and propylene oxide, embedded with LX-112 medium, and polymerized at 70°C for 48 h before sectioning.

Ultrathin sections (~80 nm) were cut with a regular diamond knife, collected on 200-mesh, uncoated copper grids, and double stained with 50% saturated uranyl acetate and 0.2% lead citrate. The sections were then examined with a JEOL-CX100 transmission electron microscope (JEOL USA, Peabody, MA) operated at 60 kV.

For postembedding immunolabeling, samples were placed in warm fixative containing 2% fresh paraformaldehyde and 0.05% glutaraldehyde in 0.1 M PBS (pH 7.4) for 10 min. The samples were trimmed, washed several times with the same PBS at 4°C, dehydrated at −25°C with ascending grades of ethanol, infiltrated with different concentrations of Lowicryl K4M medium, embedded in gelatin capsules with fresh 100% Lowicryl K4M medium, and then polymerized at −25°C with UV light for 5–7 d.

Ultrathin sections (~90 nm) were cut with a diamond knife, collected on Nickel grids coated with Formvar and thin carbon films, and labeled with specific antibodies according to the tested dilution, followed by incubation with 10 nm colloidal gold–conjugated secondary antibodies. The sections were briefly stained with uranyl acetate and lead citrate and examined with a JEOL-CX100 electron microscope operated at 60 kV (Yu et al., 1996).

Histological Analysis

Tissues were fixed in 4% formaldehyde, processed, and embedded in paraffin. Sections were cut at 5-μm thickness, mounted, and stained with hematoxylin and eosin. Sections were examined using an Axiophot microscope (Carl Zeiss, Inc., Thornwood, NY).

Results

Tensin Is Expressed Broadly in Murine Embryonic Development

To examine the expression of tensin during murine development, we first needed to isolate a mouse tensin cDNA and to raise mouse tensin antibodies. We used PCR on a pooled library of mouse lung cDNAs to isolate an 890-bp tensin cDNA. Sequence analysis revealed a strong (~90%) amino acid sequence identity between this fragment and residues 181 to 477 of the previously reported chicken tensin

cDNA (Lo et al., 1994*b*). This fragment, encompassing a 5′ segment of the tensin coding region, was subsequently used as a probe to screen the same library for additional mouse tensin clones. The cDNA insert of one clone (L52) was then used to engineer a GST fusion protein, which we subsequently used for antibody generation. Since most available tensin antibodies were raised against chick tensin (Glenney and Zokas, 1989; Kanner et al., 1990; Lo et al., 1994*b*), they either did not cross-react with mouse tensin, or they recognized the mouse protein weakly. Our tensin GST fusion protein reacted strongly with mouse tensin in tissues and on immunoblots (see below). We were now equipped with the necessary molecular tools to examine tensin expression during mouse development.

We first performed Northern blot analysis, hybridizing our mouse tensin cDNA (L52) to mouse RNAs isolated from whole embryos taken at different ages. By gastrulation, tensin RNAs were abundantly expressed (Fig. 1). At E7, a major RNA band of 10 kb and a minor band of 7 kb hybridized with the probe under stringent conditions (Fig. 1). The same probe detected a single 6.7-kb EcoRI mouse genomic fragment on a Southern blot, and a 210-bp cDNA probe complementary to a further upstream 5′ sequence of mouse tensin RNA detected the same two bands (data not shown). Thus, it is most likely that these size differences in tensin transcripts reflect either alternative usage of polyadenylation signals or differential splicing. The 10-kb RNA band corresponded most closely in size to that expected based on knowledge of the chicken tensin mRNA (Davis et al., 1991; Lo et al., 1994*b*; Chuang et al., 1995).

Tensin RNAs remained prominent at all embryonic ages examined. While expression of β-actin mRNA remained relatively constant in these embryo preparations of different ages, expression of tensin mRNAs decreased between E7 and E11 and then increased again between E11 and E17 (Fig. 1). RNAs encoding another focal adhesion protein, p130cas, followed a profile more similar to that of the β-actin control. We have not yet explored the underlying reason for the unusually high level of tensin mRNA expression at very early embryonic ages. However, in situ hybridization analyses revealed widespread tensin mRNA expression in many embryonic tissues including nasal processes, walls of the midbrain, branchial arches, centrum, heart, hepatic primordium, midgut, and lung (Fig. 2).

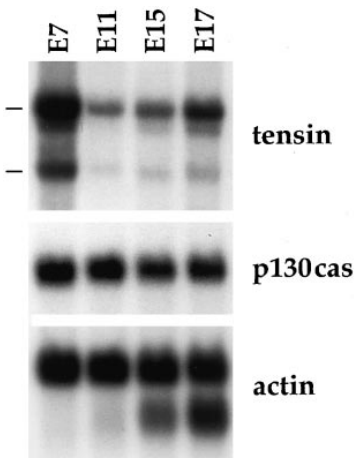

Figure 1. Tensin mRNA expression during embryonic development in the mouse. Northern blots of mRNAs isolated from mouse embryos at 7, 11, 15, and 17 d of gestation were hybridized with radiolabeled cDNA probes corresponding to tensin, p130cas, and β-actin (normalization control; the smaller sized band appearing in E15 and E17 samples corresponds to the expected size of skeletal muscle actin mRNA). Bars represent the migration of RNA molecular standards of 9.5 and 7.5 kb.

Tensin Is Expressed in a Variety of Adult Tissues

To examine tensin expression in the adult mouse, we performed Northern blot analysis on mRNAs isolated from various adult tissues. RNAs from the kidney and heart hybridized most strongly to the tensin cDNA probe (Fig. 3). Tensin-hybridizing mRNAs were also readily detected in lung, liver, and skeletal muscle, but only very weak signals were detected in the mRNAs from brain, spleen, and testis (Fig. 3). These expression patterns were very similar to those seen by immunoblot analysis using an anti-tensin antiserum (not shown). Taken together, the expression of tensin varied quite markedly among adult tissues.

Isolation of Mouse Tensin Gene and Generation of Tensin Null Mice

The tissue-specific differences in tensin RNA levels suggested the possibility that the relative importance of tensin might vary among different tissues. To explore tensin's function in vivo, we focused on using homologous recombination and embryonic stem cell technology to ablate tensin expression in mice. The 890-bp mouse tensin cDNA was used to screen a 129SV mouse genomic library. We identified one positive clone, mtensinλA, which contained a 13-kb fragment of the 5′ end of the mouse tensin gene. A partial restriction endonuclease map of this sequence is shown in Fig. 4 *A*. Sequence analyses revealed that the segment between the SpeI and the 3′ EcoRI sites encompasses the portion of the tensin gene that encodes amino acid residues 110–180 corresponding to the chicken tensin cDNA (Lo et al., 1994*b*).

The mouse tensin targeting vector was constructed from mtensinλA (Fig. 4 *A*). The ~4-kb SpeI–EcoRI fragment of the mouse tensin gene was targeted for deletion. Since tensin has two transcripts and the 210-bp cDNA fragment targeted for deletion detects both RNA forms by Northern blot analysis (see above), we predicted that the deletion of this region of the genome should result in the disruption of both transcripts. Thus, we replaced this segment with a 1.8-kb fragment containing a *pgk1* neomycin resistance gene for positive selection. The *pgk1-neo* gene was flanked 3′ with a 3-kb mouse tensin fragment and 5′ with a 2.2-kb mouse tensin fragment. A *pgk1-Herpes* thymidine kinase gene (Adra et al., 1987) was used for negative selection as outlined in Fig. 4 *A*.

Of 121 G418–gancyclovir-resistant ES clones, one was determined to have homologous recombination, and this clone was eventually transmitted to germline (see Materials and Methods). Heterozygous mice were interbred to produce litters that included homozygous offspring. Southern blot analysis of mouse DNAs isolated from the tails of these offspring revealed the expected three genotypes

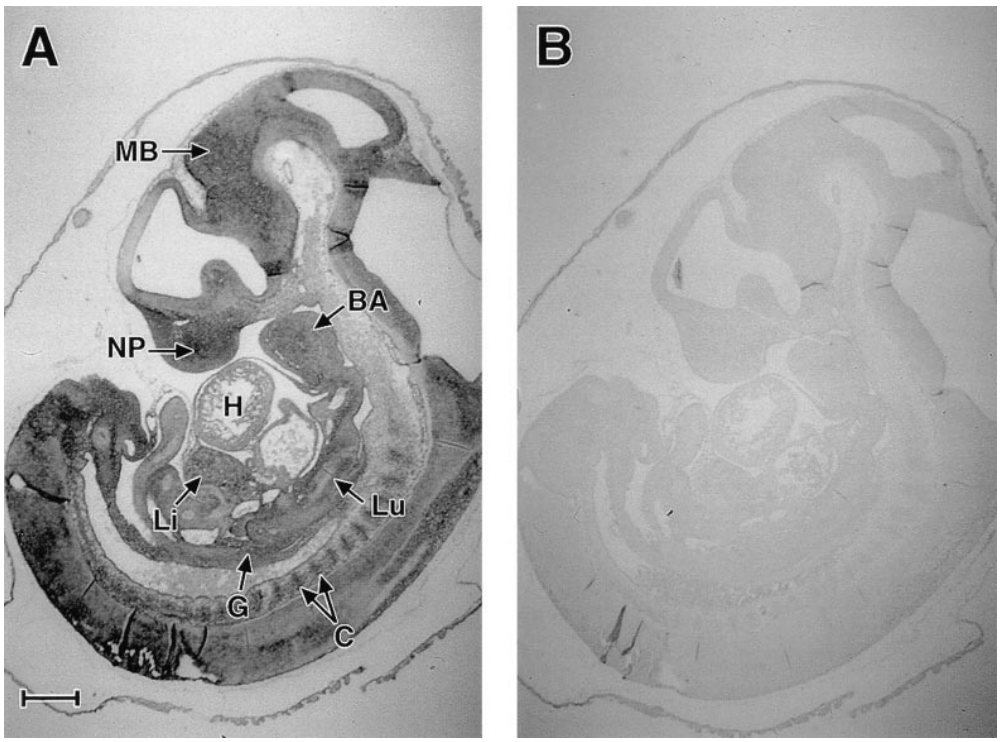

Figure 2. Expression of tensin mRNA in E10 mouse embryos. Sagittal paraffin sections (5 μm) of E10 mouse embryos were hybridized with a 1,200 nucleotide, digegoxygenin-labeled antisense tensin cRNA probe (*A*). No hybridization was detected with the corresponding sense-strand probe (*B*). *MB*, wall of the midbrain; *NP*, nasal process; *BA*, branchial arch; *H*, heart; *Lu*, lung; *C*, centrum; *G*, midgut; *Li*, liver. Bar, 420 μm.

(33+/+, 53+/−, 25−/−), as judged by diagnostic probes for the correct 5′ and 3′ homologous recombination events (Fig. 4 *B*). In addition, only a single genomic band of the expected size was shown to hybridize to the neomycin probe, suggesting that no additional recombination events had occurred.

To assess whether the targeted homologous recombination event had resulted in the loss of tensin expression, we used our monospecific mouse anti–tensin antisera (see Materials and Methods) to conduct immunoblot analysis on total proteins extracted from cultured fibroblasts that we derived from the skin of our mice. As shown in Fig. 4 *C*, the anti-tensin antibody labeled a single band of ~200 kD in fibroblast protein extracts prepared from +/+ and +/− mice, but not from those of −/− mice. This result confirmed the monospecificity of our mouse anti–tensin antibody and also verified that the targeting event to disrupt the tensin gene was successful.

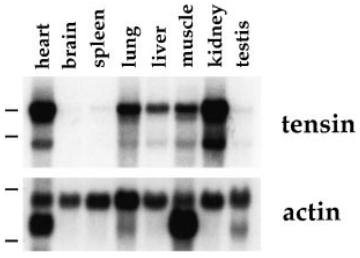

Figure 3. Expression of tensin mRNA in adult tissues. A Northern blot of mRNAs from the adult mouse tissues indicated was hybridized sequentially with radiolabeled cDNA probes corresponding to tensin and β-actin. Bars represent the migration of RNA molecular standards of 9.5, 7.5, 2.4, and 1.4 kb.

Tensin Null Mice Display Striking Abnormalities in Their Kidneys

Tensin −/− mice appeared normal at birth. As judged by external appearance, body weight, and general behavior, the developing postnatal tensin null mice did not seem to differ from their wild-type or heterozygote littermates. At 2 mo old, animals were killed for further analysis. Gross anatomical examination of the brain, liver, heart, spleen, stomach, skin, lung, eyes, and intestine revealed no obvious abnormalities. In contrast, the kidneys of tensin null animals exhibited significant and consistent abnormalities. The defects were bilateral and genotype related: they were not found in any +/+ or +/− mice examined. We have not yet examined whether the defects in the −/− mice vary with mouse strain; as yet all our findings are confined to an analysis of the 129sv/C57BL6 hybrid knockout animals.

Kidneys from mutant mice were pale and had a granular appearance on their surface (Fig. 5 *A*). Often, the −/− kidneys were slightly larger than age-matched wild-type kidneys. When hemisected, the +/+ kidneys always displayed a dark reddish brown cortex, i.e., the region of the kidney that contains the proximal and distal tubules and the glomeruli (Fig. 5 *B*). In +/+ kidneys, this region was readily distinguishable from the lighter medulla, where the collecting ducts and Henle's loops reside (for reference see diagram in Fig. 6). This distinction in coloring within the wild-type kidneys was notably less prominent in the −/− kidneys (Fig. 5 *B*). In addition, the renal pelvis opening was markedly enlarged in many of the kidneys from tensin null mice. In severe cases, cortex and medulla regions were often so compressed that the mutant kidneys were nearly empty (Fig. 5 *B*).

Histologic examination of sections of kidneys from tensin null animals revealed various degrees of cystic de-

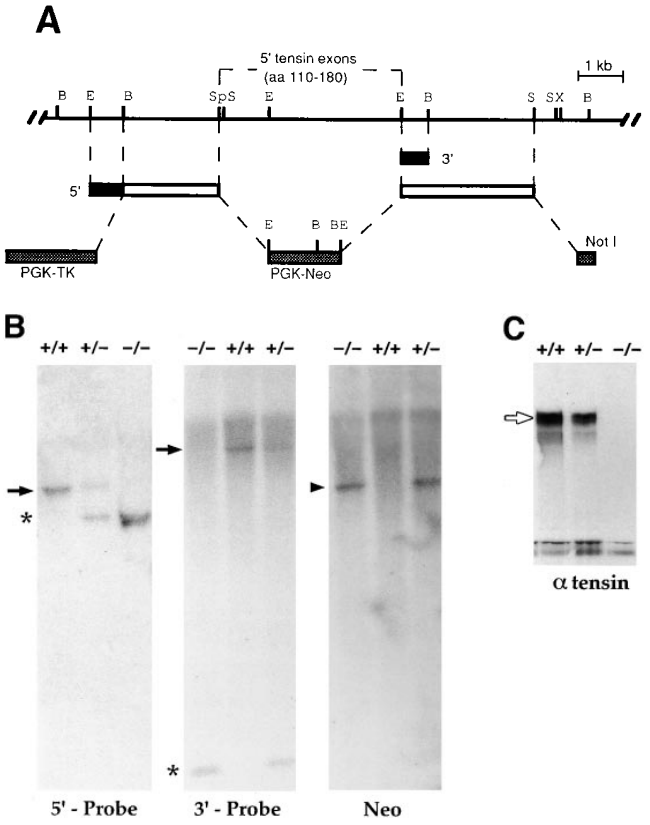

Figure 4. Disruption of the tensin gene in embryonic stem cells and in mice. (*A*) Targeting vector and homologous recombination at the tensin locus. Shown is a partial restriction map of a portion of the mouse tensin gene. (*Open boxes*) 5′ and 3′ flanking sequences used for targeting; (*black boxes*) 5′ and 3′ genomic DNA probes used for Southern blot analysis; (*PGK-Neo* and *PGK-TK*) neomycin resistance and Herpes thymidine kinase genes, under the control of the phosphoglycerate kinase 1 promoter, used for positive and negative selection, respectively. *B*, BamHI; *E*, EcoRI; *Sp*, SpeI; *S*, SacI; *X*, XhoI. (*B*) Southern blot analyses of DNA isolated from the tails of +/+, +/−, and −/− mice. Mouse tail DNAs were digested with restriction endonucleases EcoRI (*left*) or BamHI (*middle* and *right*) and resolved by electrophoresis through 0.8% agarose gels. After transferring to nitrocellulose paper, blots were hybridized with radiolabeled cDNA probes corresponding to the 5′ and 3′ fragments indicated in *A*, and to the *PGK-Neo* gene (5′ EcoRI–BamHI fragment) as indicated. (*Asterisks*) Bands expected for a successful homologous recombination event (2.8 kb, 5′ probe; 0.4 kb, 3′ probe); (*arrows*) bands expected for the wild-type genome (4 kb, 5′ probe; 6.8 kb, 3′ probe); (*arrowhead*) band for neomycin probe (3.8 kb). (*C*) Immunoblot analysis of tensin protein in fibroblasts derived from +/+, +/−, and −/− 15-d mouse embryos. Fibroblasts were cultured from the skin of 15-d mouse embryos. Whole-cell lysates (30 μg) were subjected to electrophoresis through a 7% polyacrylamide SDS gel, and then transferred to nitrocellulose. After staining with Ponceau S to confirm equal loading of proteins (not shown), the blot was reacted with an anti-tensin antiserum. The blot was developed with enhanced chemiluminescence (Amersham Corp., Arlington Heights, IL). A single 200-kD band, corresponding to the size of mouse tensin, was detected in protein samples from wild-type and heterozygote fibroblasts, but not from the tensin null fibroblasts.

fects that were not seen in control sections (Fig. 5, *C–H*). These defects ranged from extremely dilated cysts in the cortex and medulla of severely affected kidneys (Fig. 5, *D* and *F*) to small cysts in the cortex of the less affected organs (Fig. 5 *H*). Most small cysts arose from proximal tubules, as suggested by Periodic Acid-Schiff staining and as further judged by EM (see below). Upon closer inspection of these cysts, it appeared that they derived from an expansion of the tubular lumen (Fig. 5 *H*). This was less obvious in the larger cysts, where gross distortions often precluded identification of the origin of cells that lined the cysts.

Higher magnification revealed additional abnormalities in the kidneys from the tensin null mice (Fig. 5, *I–N*). Some cysts contained atypical casts, i.e., amorphous materials, which seemed to be noncellular (Fig. 5 *I*, see also *double arrows* in 5 *F*). Many glomeruli displayed enlarged Bowman's spaces, i.e., the regions where small molecules filtered from the blood will normally collect and pass into the proximal tubules (Fig. 5 *F*, *single arrow*, and 5 *J*, *double arrows*). In addition, the epithelial cells that surround each glomerulus were often enlarged and cuboidal (Fig. 5 *L*, *arrowheads*), in contrast with the flattened, barely visible simple squamous epithelium that surrounded control glomeruli (Fig. 5 *K*). In the most severely affected regions of the −/− kidneys, signs of focal segmental glomerular sclerosis were found. These highly abnormal areas of the glomerulus are thickened and appear to contain extracellular depositions, which could be an increase in mesangial matrix (Fig. 5 *M*, *arrowhead*). Finally, interspersed throughout the affected kidneys were focal interstitial inflammatory infiltrates (Fig. 5 *N*, *arrowheads*). Taken together, these histological findings suggested strongly that large regions of the kidneys of tensin null mice were not functioning properly, and that fluid flow from the glomeruli to the collecting ducts was aberrant.

The pale and granular surface of −/− kidneys was a consistent feature of tensin null animals and was usually evident by ~4–8 wk after birth. In addition, very small cysts in the −/− kidneys could often be detected as early as 1–2 wk postnatally, while the gross abnormalities in the glomeruli were often not seen until the adult stage. In general, older animals had more severe kidney defects. However, this was not always the case, as some older mice, i.e., >6 mo old, displayed only mild cystic defects (but kidneys were always pale). Conversely, some juvenile mice as young as 2 wk old sometimes possessed kidneys with an enlarged renal pelvis space. Taken together, these data suggest that the kidney abnormalities occurring in these animals were not reflective of a specific developmental or temporally defined defect. Rather, the deterioration appeared to be slow, progressive, and triggered by some as yet unidentified stress, initiated by the absence of tensin. This said, we cannot exclude the possibility that the mixed genetic background (129sv/C57BL6) played a role in the variable onset time of kidney degeneration that was observed in the tensin null progeny.

Despite the dramatic histological abnormalities in the −/− kidneys, the tensin null mice most often appeared clinically normal. To date, only three of 44 mice (18 wk, 8 mo, and 9 mo of age) have become visibly ill in a fashion that might be consistent with kidney failure. The 18-wk-old female mouse had delivered once with two pups (one born

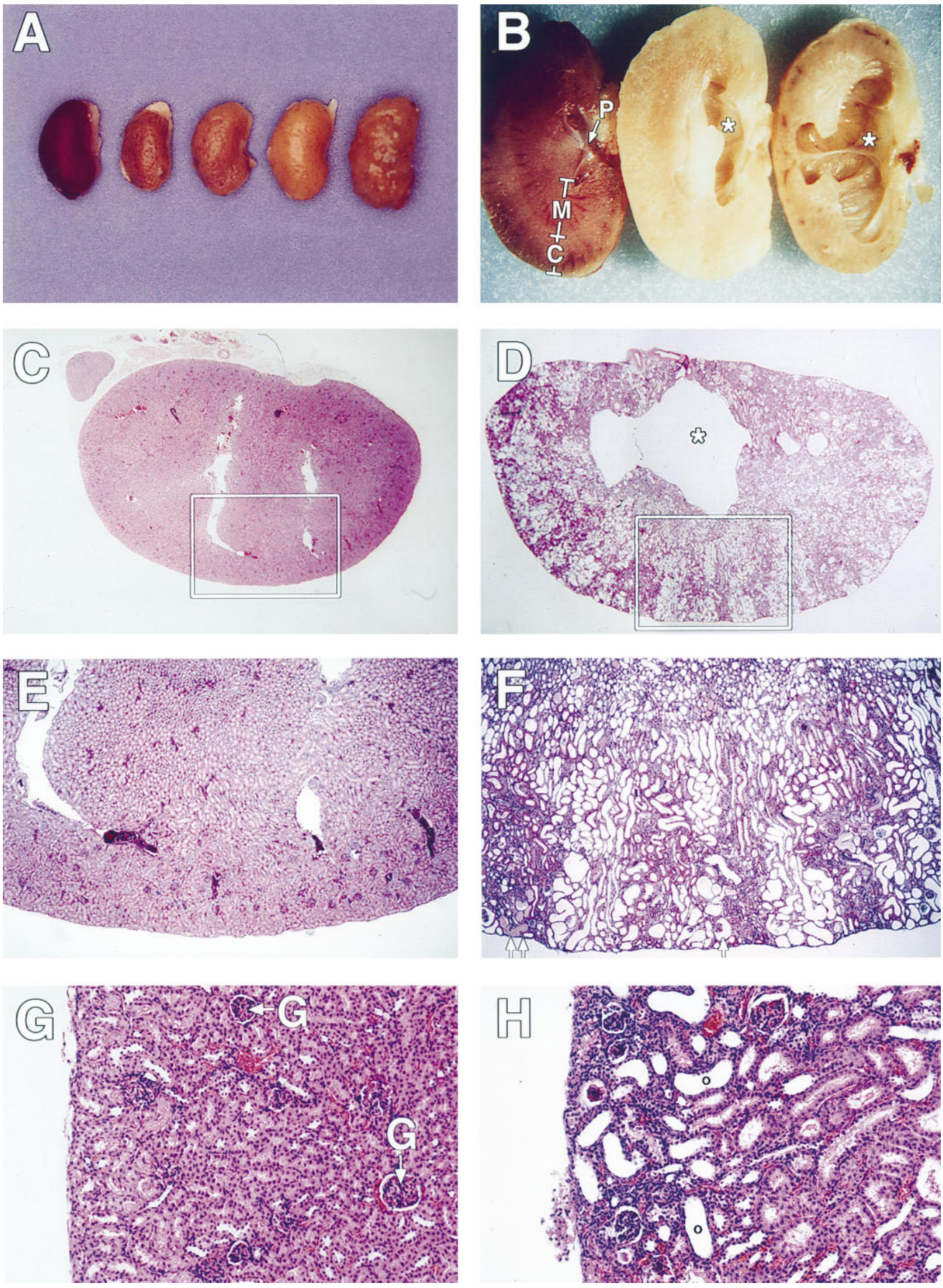
A
B
P
T
M
C
C
D
E
F
G
G
G
H

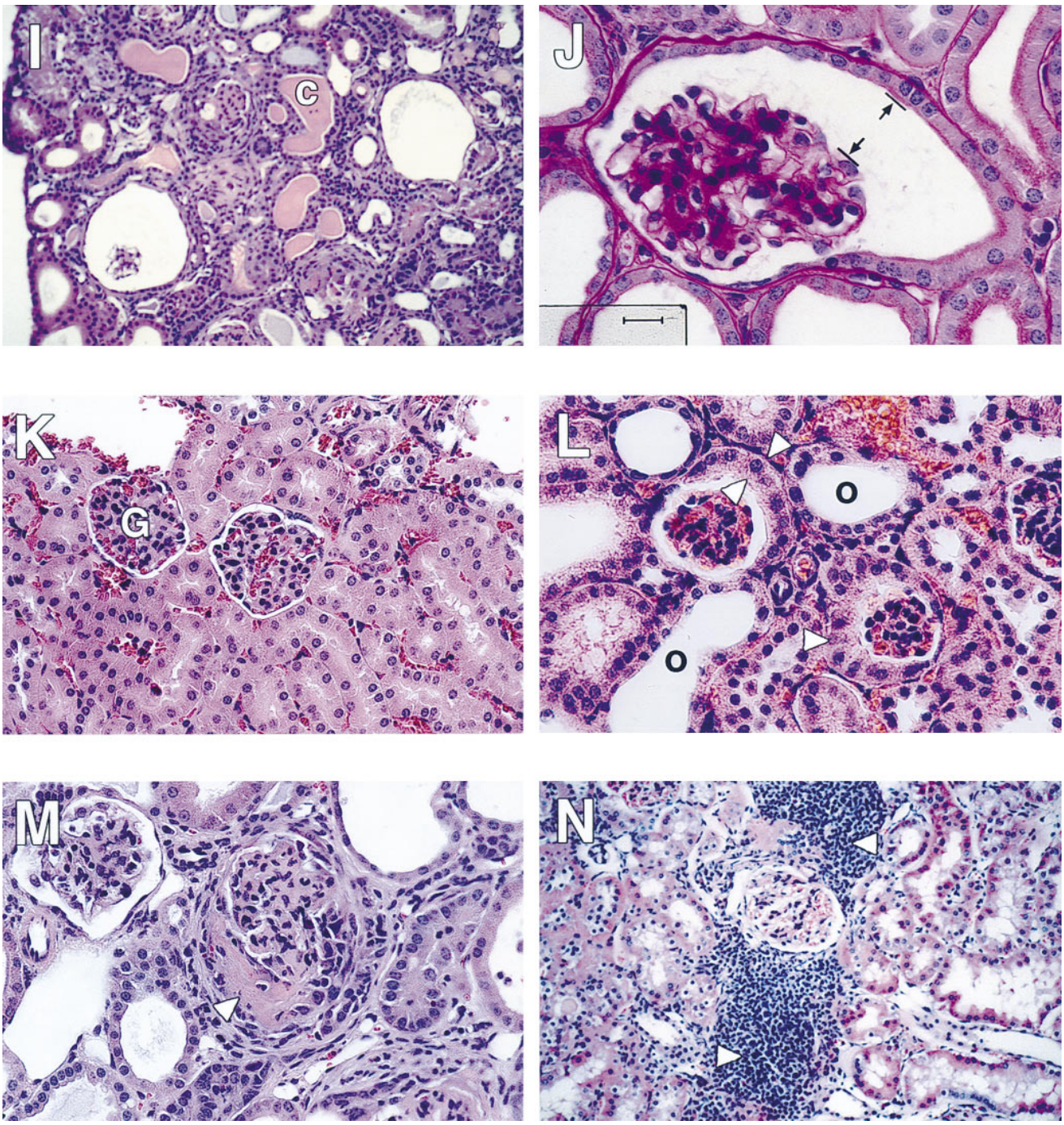

Figure 5. Abnormalities in the overall appearance and histopathology of the kidneys of tensin −/− mice. (*A*) Wild-type or tensin null mice were killed at various ages, and their kidneys were isolated and examined. Shown are representative kidneys from (*left to right*): 23 wk +/+, 6 wk −/−, 14 wk −/−, 28 wk −/−, and 36 wk −/− mice. Note the pale color of the tensin null kidneys at all ages. (*B*) Shown are representative hemisected kidneys from (*left to right*): 23 wk +/+, 28 wk −/−, and 14 wk −/− mice. (*C–F*) Kidneys from 18-wk-old tensin null mice and their control wild-type littermates were placed in formaldehyde fixative, sectioned (5 μm), and stained with hematoxylin and eosin. Shown are representative sections from the kidneys of +/+ (*C*; box denotes region magnified in *E*) and −/− (*D*; box denotes region magnified in *F*) mice. Note the enlarged space, corresponding to the renal pelvis, in the knockout (*asterisk* in *D*). Note the presence of numerous cysts in the −/− kidney sections, a typical feature of the knockout animals. (*G–I*) Kidneys from 4-wk-old tensin null mice and their control littermates were fixed and stained as outlined above. Shown are representative sections of (*G–H*) the cortical regions of +/+ (*G*) and −/− (*H*) kidneys; note again the prevalence of cysts (*open circles*) in the knockout kidney. *G*, glomeruli. (*I*) Section of −/− cortex to illustrate cysts containing amorphous materials (*C*), often referred to as casts (*double arrow* in *F*). (*J*) Section of −/− glomeruli, revealing large space in Bowman's space (*double arrow*), commonly seen when fluid backs up in the capsule as a result of a malfunctioning of the kidney (see also *arrow* in *F*). (*K*) Glomeruli (*G*) from wild-type kidney; note the normal spacing surrounding Bowman's space. (*L*) Glomeruli from tensin null kidney; note that these glomeruli were surrounded by atypical cuboidal epithelial cells with a prominent cytoplasm (*arrowheads*), rather than the normal thin flattened epithelia, barely visible in the control glomeruli. (*Open circles*) cysts. (*M*) Glomerulus from a tensin −/− kidney, surrounded by a highly irregular epithelium; also note what appears to be extracellular material, possibly collagen, similar to that seen in focal segment glomerular sclerosis in humans. (*N*) Region from a tensin null kidney, depicting marked signs of focal interstitial inflammatory infiltrates. Bar: (*C* and *D*) 740 μm; (*E* and *F*) 400 μm; (*G* and *H*) 100 μm; (*I* and *N*) 50 μm; (*K–M*) 25 μm; (*J*) 17 μm.

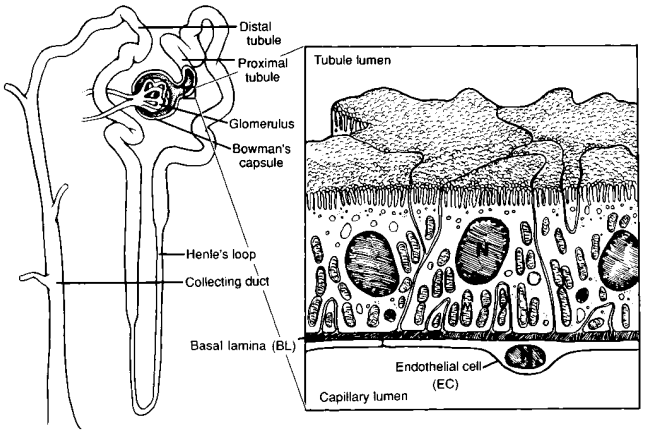

Figure 6. Schematic illustration of a nephron unit of the kidney and of the epithelium of a proximal tubule. The kidney comprises more than a million nephrons, the functional unit of the kidney. Blood enters the glomerulus at the start of each nephron. After filtration to remove proteins and cells, the remaining fluid, composed largely of water and small molecules, such as salts, amino acids, and glucose, passes through the Bowman's capsule surrounding the glomerulus and into the proximal tubule. Here most of the nutrients are reabsorbed across the polarized epithelium of the tubule (boxed area is enlarged to illustrate the epithelium at right). The portion of fluid that is not reabsorbed continues to pass through the kidney tubules, where it exits as urine. The epithelium of the proximal tubule differs from the distal tubule epithelium in that it contains a thick brush border for high efficiency absorption of small molecules. The basal side of the epithelium undulates to form what is called a basolateral labyrinth, which encases the numerous mitochondria necessary to provide the energy for transport. Separating the basal surface of the epithelium from the endothelial walls of the capillaries is a basement membrane composed of ECM. Integrin-mediated attachment of the basal surface to the underlying ECM is thought to be essential for polarizing the epithelium and for enabling proper transport to take place. The glomeruli and the proximal and distal tubules reside in the outermost region, i.e., cortex, of the kidney; the collecting ducts, located in the medulla of the kidney, pass urinary fluid into the renal pelvis.

dead). In comparison with her littermates, her body weight was less (19 g vs 21 g), her kidneys were double their normal size (0.25 g and 0.26 g vs 0.12 g and 0.12 g), and her liver was smaller (0.5 g vs 1.0 g). Spleen, heart, and lung sizes were similar to those of her littermates. The 8-mo-old female (24 g) delivered once and similarly displayed enlarged kidneys (1.0 g and 0.6 g) that were filled with fluid. In this case, the heart appeared hardened, but it was not analyzed further. Finally, the 9-mo-old male mouse was thin (19 g), and both kidneys were enlarged, displaying cysts on their surfaces and large renal pelvic cavities. This mouse was the most affected, with many organs showing signs of deterioration. The chest of this animal was full of fluid, and signs of scarring were seen on the heart. Since we have not yet been able to generate sufficient numbers of tensin null mice that are overtly ill, we are not able to say unequivocally whether the ill mice in the colony suffer or die from kidney failure. However, we have conducted blood tests on 15 clinically normal, adult tensin null mice and 26 of their control littermates. Glucose levels were largely normal (161 ± 30 mg/dl −/− vs 164 ± 25 mg/dl control), as were creatinine levels (0.33 ± 0.08 mg/dl −/− vs 0.22 ± 0.04 mg/dl control) and blood urea nitrogen levels (36 ± 10 mg/dl −/− vs 21 ± 4 mg/dl control). In contrast, the Bcl-2 null mice displaying full-blown polycystic kidney disease have creatinine levels (0.77 ± 0.54 mg/dl −/− vs 0.19 ± 0.07 mg/dl control) and blood urea nitrogen levels (116 ± 87.6 mg/dl −/− vs 21 ± 5 mg/dl control) that are considerably abnormal (Veis et al., 1993). These findings are consistent with the notion that only a small fraction of the kidney needs to be healthy to provide a seemingly normal urine output (Junqueira et al., 1995; Tisher and Brenner, 1994).

Tensin Is Expressed in the Epithelial Cells of Kidney Tubules

Since kidney was one of the mouse organs displaying a high level of tensin mRNA and protein, and since it was the only tissue where major pathology was detected, we were interested in where tensin was localized within the kidney. To answer this question, we performed immunohistochemistry on tissue sections taken from a mouse kidney. Antibodies monospecific for tensin showed staining in many areas within the kidney, including the collecting tubules within the medulla; however, staining was most concentrated over the proximal and distal tubules in the cortex region (Fig. 7).

Detection and Localization of Tensin at Cell–Matrix Junctions of Kidney Tubules

The presence of tensin in the tubule epithelia was interesting, given that tubular cysts were an early sign of pathology in the tensin null mice. To further localize tensin within the kidney tubule cells, regular and immunoelectron microscopy were performed on wild-type mouse kidneys. Prominent antitensin labeling was detected at the basal membrane of the tubular and endothelial cells (Fig. 6, schematic; Fig. 8 *A*, proximal tubule cell; Fig. 8 *B*, antitensin labeling, restricted to the base of the tubule cell). Periodically along the base of the basolateral labyrinth of each kidney tubule cell were sites of markedly heavy antitensin labeling (Fig. 8 *B*, *arrows*; see also *inset*). In addition, numerous smaller clusters of antitensin labelings were evident. The presence of small and large clusters of gold particles at the base of the epithelium from antitensin labeling suggested that two kinds of focal adhesion complexes might exist in the kidney tubule cells. Support of this hypothesis came from seeing similar labeling with an antibody against p130cas, another focal adhesion protein (data not shown).

A more diffuse antitensin labeling was seen at both edges of the basal membrane (Fig. 8 *B*). This labeling was not present in control tissue labeled with secondary antibodies alone. Thus, despite the fact that the labeling seemed to be extracellular rather than intracellular, we think it most likely that this labeling reflects an intracellular residence of tensin at these locations. Perhaps slight retraction of cells during the fixation process left the leading edges of the tubule and endothelial membranes within a region that appeared by ultrastructure to be pure basal membrane. Antitensin labeling was not detected elsewhere within the tubule cells of the kidney, consistent with the notion that focal adhesion and cell–substratum contacts play an exclu-

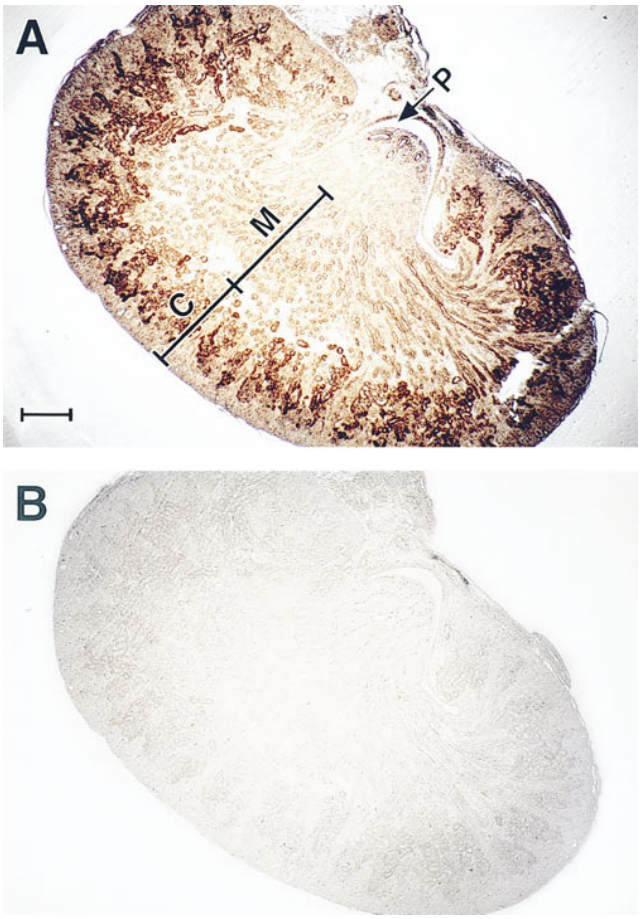

Figure 7. Tensin protein is expressed in the epithelial tubules of the mouse kidney. A kidney from a wild-type mouse was formaldehyde fixed, processed, embedded in paraffin, and sectioned sagitally. Sections (5 μm) were then labeled with primary antibodies against mouse tensin, followed by enhancement with immunogold-conjugated goat anti–rabbit IgG secondary antibodies (*A*). In the control section in *B*, the preimmune serum was used in the labeling reaction. *C*, cortex, containing the glomeruli and proximal/distal tubules (note strong labeling over the tubules); *M*, medulla, containing the collecting ducts and Henle's loops (note weaker labeling over the collecting tubules); *P*, renal pelvis. Bar, 260 μm.

sive role at the base of the basolateral labyrinth, and not at the lateral or apical regions of the tubule cells.

Focal Adhesions Are Present in Seemingly Normal Tubules of Tensin Null Kidneys but Are Missing in the Cystic Tubular Cells

In a normal kidney, the proximal tubules are lined by a simple cuboidal epithelium. The apex of each epithelial cell possesses abundant microvilli that form a brush border (see Fig. 6). The basal portion of the cell has abundant membrane invaginations, referred to as the basal lateral labyrinth. Numerous elongated mitochondria are concentrated within this region of each cell, and the locations of mitochondria and increased cell membrane invaginations are characteristic of cells engaged in active ion transport (Junqueira et al., 1995). Throughout the histologically unaffected or mildly affected areas of the kidneys of tensin null mice, the cuboidal epithelium of the proximal tubules was ultrastructually normal (Fig. 9 *A*). This was in striking contrast with the severely affected regions, where microvilli were largely deteriorated, mitochondria were less organized and less abundant, and the basal membrane displayed fewer invaginations (Fig. 9 *B*). Many cells exhibited irregularities in cell shape, and the epithelium often appeared to be less polarized. Despite these aberrations, tight junctions could be detected between the defective cells, suggesting that polarization was not completely lost.

Most interestingly, in the more mildly affected regions, immunogold labeling with antibodies against p130cas displayed both large (not shown) and small (shown) clusters of gold particles at the base of the basal lateral labyrinth (Fig. 9 *C*). This labeling was indistinguishable from that which we had seen with antitensin (Fig. 8 *B*) and with anti-p130cas (not shown) in the proximal tubules of the wild-type kidney. In contrast with the normal-looking proximal tubules, the dilated, cystic proximal tubules of tensin null mice displayed an overall paucity of anti-p130cas labeling, even when some cell–substratum adhesion still occurred (Fig. 9 *D*).

In regions where the tubules showed signs of cyst formation, labeling with antibodies to the sodium-potassium ATPase was also significantly reduced (Fig. 9 *F*, compare with largely unaffected region in Fig. 9 *E*). This finding was interesting because this protein typically localizes in the membrane, along the basolateral zones of the proximal epithelial cells (Fig. 9 *E*). Thus, the reduction in epithelial polarity was not restricted to the basal surface of the cells, but rather extended to lateral and apical surfaces as well. Given the localization of tensin in these cells, we presume that the abnormalities in lateral and apical markers are secondary and arise as a consequence of a change at the basal surface, initiated by the loss of tensin.

Although we detected mild antitensin labeling at the interface between podocyte foot processes and the basement membrane of wild-type kidney glomeruli, no significant ultrastructural changes were detected in the tensin −/− glomeruli. Moreover, we did not detect fusions of foot processes nor separations of podocytes from their underlying basement membranes (data not shown).

Tensin −/− Female Mice Produce Few Live Pups

Although both male and female tensin −/− mice are fertile, our homozygous mutant females mated to homozygous mutant males have produced few live offspring. Thus far, in 14 matings of homozygous females and males, only nine have produced offspring, and the average litter size has been only three pups (Table I). In contrast, crosses between homozygous males and either wild-type or heterozygous females have produced normal litters, ranging from seven to nine pups. These data suggest a defect in the breeding potential of homozygous female mice. To further explore this issue, we killed one pregnant −/− female to examine her embryos at 15 d of gestation: three were alive, one was dead, and one had been adsorbed. While additional studies will be necessary to determine the mechanism underlying this deficiency, our findings suggest that normal fertilization occurs, although a higher incidence of spontaneous abortion may be taking place in these mothers.

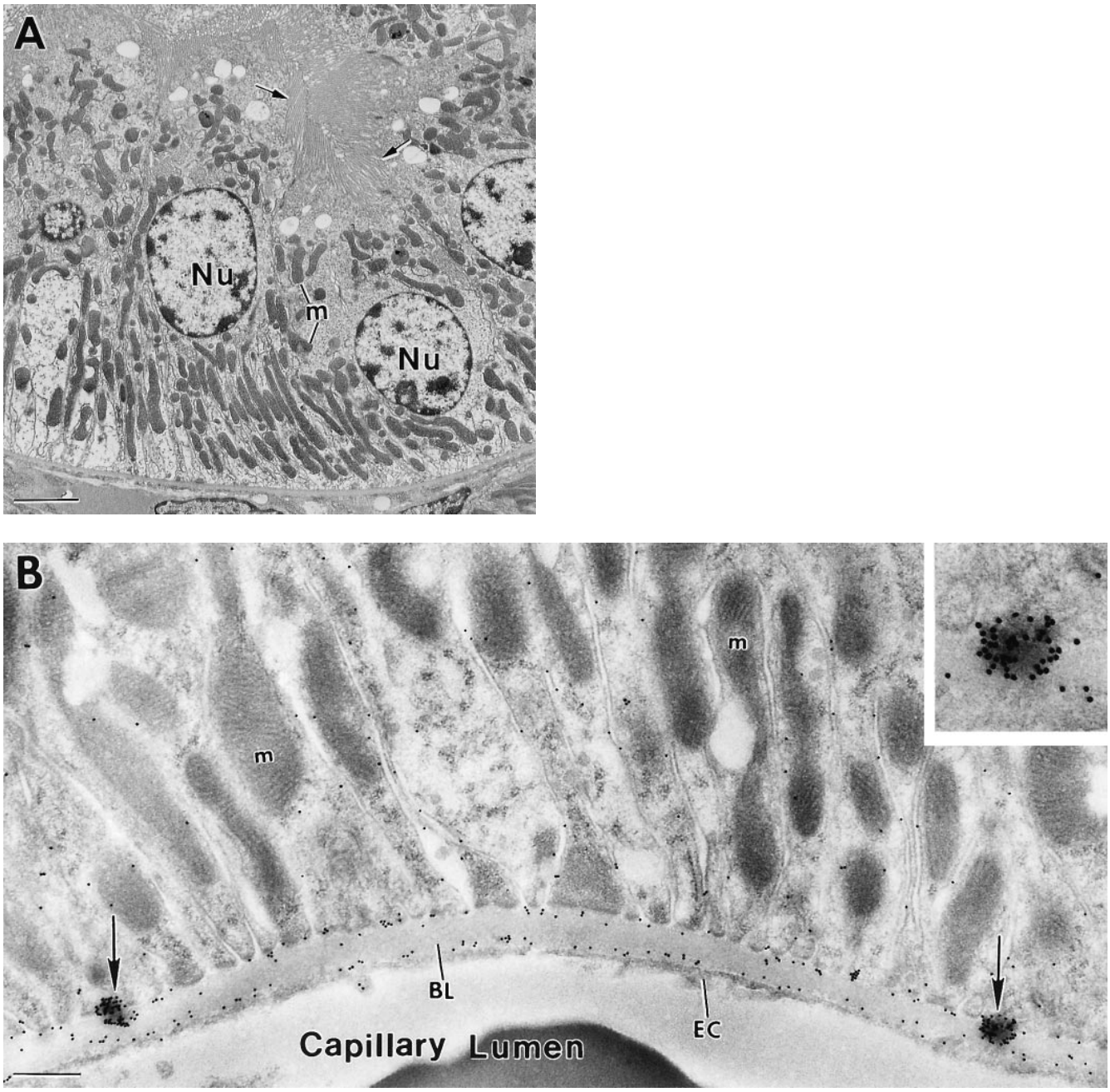

Figure 8. Immunoelectron microscopy reveals tensin in two types of focal contacts along the basal surface of wild-type kidney tubules. Kidneys from wild-type mice were processed for regular or immunoelectron microscopy. Shown are ultrathin sections of epithelial cells from the proximal tubules. (*A*) Polarized epithelial cells illustrating the presence of invaginations at the base of the epithelium, adjacent to the basal lamina and numerous microvilli (*arrows*) at the apical surface. Note the numerous mitochondria (*m*), reflective of transport activity, near the basal end of the cells. *m*, mitochondria; *Nu*, nucleus. (*B*) Epithelial cells labeled with antibodies against tensin. Note two very large clusters of dense grains at the base of the epithelium (also at higher magnification in *inset*), next to the basal lamina (*BL*). Note also more numerous smaller clusters of grains near the tips of the epithelial invaginations, where the epithelium made contact with the basal lamina. Both types of labelings were seen throughout the tissue, wherever the tubule epithelium was in contact with the underlying basal lamina. Similar labelings were also seen with antibodies against p130cas, another focal adhesion protein (not shown). Note we routinely observed gold particles in regions that appeared to be within the basal lamina; this (and other) labeling was specific for antibodies against focal adhesion proteins. We presume that the highly localized, but seemingly extracellular, labeling is an artifact, perhaps generated by a slight retraction of the cell's surface during fixation. *EC*, endothelial cell. Bar: (*A*) 3 μm; and (*B*) 0.5 μm.

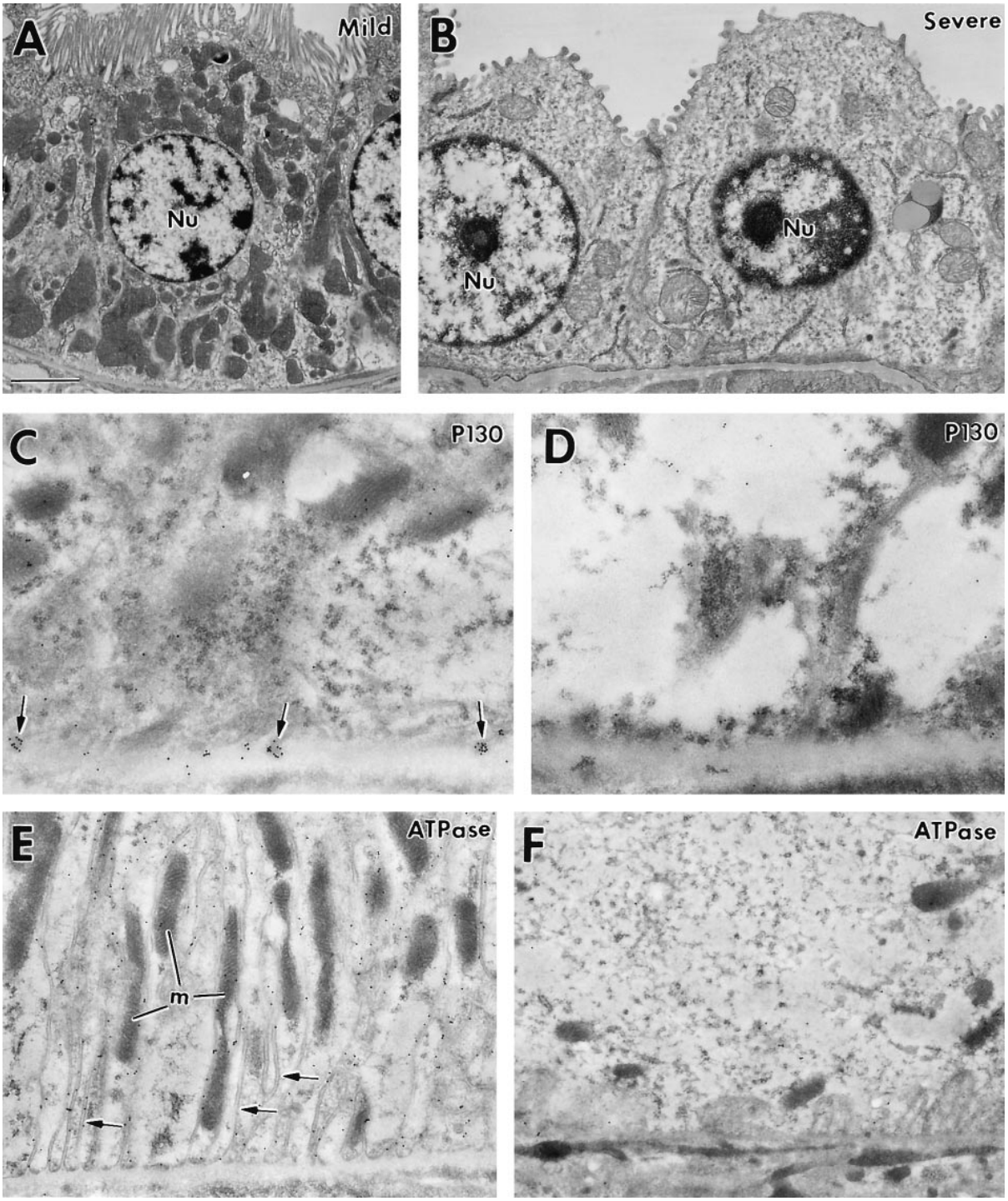

Figure 9. Immunoelectron microscopy reveals the presence of focal adhesions in seemingly normal areas of the tensin null kidney tubules and the absence of focal adhesions in cystic tubules. Kidneys from tensin null mice were processed for regular or immunoelectron microscopy (see Materials and Methods). Shown are ultrathin sections of epithelial cells from the proximal tubules of mildly affected or seemingly unaffected areas (*A*, *C*, and *E*) and of severely affected areas (*B*, *D*, and *F*). (*A*) Proximal tubule cells from a mildly affected region. Note that the epithelium is polarized, with numerous microvilli on the apical surface. In some regions such as this one, the only abnormality detected was fewer undulations of the basal membrane; however, such differences were not always seen. (*B*) Proximal tubule cells from a severely affected region. Note that only a few residual microvilli remain, and the epithelium shows few signs of polarization. (*C–F*). Tubular epithelial cells labeled with antibodies against p130 (*C* and *D*). Note that the mildly affected epithelial cells still display labeling of focal adhesions (*arrows* in *C*). Occasional large focal contacts similar to those depicted in Fig. 8 were also seen. Note the absence of significant labeling in the severely affected regions, suggestive of a loss of focal adhesions. (*E* and *F*). Tubular epithelial cells labeled with antibodies against the sodium-potassium ATPase (*E* and *F*). Note that the mildly affected regions still showed labeling of the basolateral surface, as is typical of wild-type controls (not shown). Note the absence of significant labeling in the severely affected regions, suggestive of a loss of cell polarity. *Nu*, nucleus, *M*, mitochondria. Bar: (*A*) 2.3 μm; (*B*) 1.3 μm; (*C*) 0.6 μm; (*D*) 0.4 μm; (*E* and *F*) 0.7 μm.

Discussion

Inactivation of tensin gene expression by targeted ablation has unveiled a specialized role for tensin in the kidney. Given the widespread importance of focal adhesions in development and differentiation, and the fact that many focal adhesion molecules including α5 and β1 integrins and focal adhesion kinase (Fassler and Meyer, 1995; Furuta et al., 1995; Stephens et al., 1995) lead to early embryonic lethality when targeted for removal, we were not expecting live homozygous pups when we crossed heterozygous mice. Moreover, since (*a*) tensin has an SH2 domain and is one of the few known targets for tyrosine phosphorylation in the focal adhesion complex, (*b*) tensin associates with the actin cytoskeleton in several different ways, and (*c*) we discovered that tensin is broadly expressed in embryonic development and in a variety of postnatal tissues, we expected that the loss of tensin would be felt by many different cell types and at many stages of development and differentiation.

Our results demonstrated that tensin is not necessary for mouse embryogenesis. While we cannot rule out the possibility that a related protein compensates for tensin in embryogenesis, a variety of different tensin cDNA probes and antibodies have failed thus far to suggest the existence of another tensin family member. This said, other actin-binding proteins have been identified at focal adhesions, and these may perform similar functions to tensin in tissues besides the kidney.

Given the results of our knockout, it was intriguing that the highest levels of tensin we detected were in the kidney and heart. The appearance and function of the tensin −/− heart seemed normal, although additional studies will be necessary to determine whether subtle defects might be present. In contrast, the kidneys from our postnatal tensin null mice displayed abnormalities that seemed to become progressively more pronounced with age. Tensin null kidneys were uniformly pale, ranging from brown to light yellow, but never the reddish brown that is characteristic of normal kidneys. Since kidney color is reflective of the flow of blood and/or its components, the paleness of the tensin null kidneys immediately suggested that fluid flow through the kidneys was compromised in our animals.

The rough and granular surface of the kidneys of our tensin null mice was likely due to the presence of numerous cysts under the surface. Most, but not all, of these mutant kidneys also possessed an enlarged renal pelvic cavity, and, in some cases, only a very thin parenchymal layer remained. Since we found compressed cortical and medullar regions in mildly affected kidneys, the hollow kidneys that we saw in severe instances most likely arise from enlargement of the renal pelvis, a feature that is often reflective of obstruction of fluid flow in the kidney.

Table I. Summary of Litter Sizes in Different Matings

Male	×	Female	Total live pups (litters)	Average litter size (SD)
Homozygous	×	Homozygous	25 (9)	2.9 (1.96)
Homozygous	×	Wild type	28 (3)	9.3 (1.15)
Heterozygous	×	Heterozygous	111(15)	7.5 (1.84)
Wild type	×	Wild type	51 (6)	8.5 (1.38)
Wild type	×	Homozygous	2 (1)	2

A partial block in urine flow could certainly lead to an enlargement of the renal pelvis and eventual parenchymal loss, concomitant with the loss of color in the kidney. To some extent, this condition resembles that seen in the human kidney disease known as hydronephrosis, where dilation of the renal pelvis and calyces are associated with progressive atrophy of the kidney resulting from obstruction of the urinary tract (Tisher and Brenner, 1994). Hydronephrosis can be congenital or acquired, unilateral or bilateral, partial or complete; it tends to remain asymptomatic until a very late stage in progression (Tisher and Brenner, 1994).

Several observations suggest that dilation of the proximal tubules might initiate the kidney defects that we see in tensin mutant mice: (*a*) in mildly affected kidneys, dilated tubules were concentrated in the cortex of the kidneys; (*b*) tensin appeared to be most highly expressed in the cortical tubules; (*c*) glomerular abnormalities were not present, except in situations where tubular cysts were also prevalent; and (*d*) the majority of the dilated tubules displayed residual microvilli, exclusive to the proximal tubules of the kidney.

Based on our immunoelectron microscopy, we know that tensin is localized at the cell–matrix junctions of the tubular cells in kidneys. Our labeling patterns revealed the existence of two kinds of in vivo focal adhesion complexes. We have observed similar labeling patterns at the basement membrane junction in the epidermis (unpublished results), indicating that these hitherto unrecognized junctions are likely to be broadly present in a variety of epithelia. The relative importance of such junctions in kidney tubular cells vs the epidermis or other stratified epithelia may be rooted in the fact that kidney epithelia do not possess hemidesmosomes, which are the major forms of cell–substratum attachment in stratified epithelia (Dowling et al., 1996; Georges-Labouesse et al., 1996; Van der Neut et al., 1996).

We cannot yet fully explain how the loss of tensin might lead to an imbalance of fluid flow in the kidney. One possibility consistent with our knowledge of how tensin might function is that, without tensin, focal adhesions might be weakened in the kidney, leading to the loss of polarity seen in some tubular cells. The loss in polarity might compromise the transport of water and other small molecules across the proximal tubules, leading to cyst formation and a partial block in urine flow, resulting in an increased pelvic pressure.

A number of lines of evidence point to the importance of cell–matrix attachment in epithelial polarity and directional transportation of molecules in the proximal tubules of the kidney (Klein et al., 1988; Sorokin et al., 1990; for review see Eaton and Simons, 1995). These tubules play a critical role in reabsorption of small molecules that are passed through the glomeruli. Proximal tubules are responsible for reabsorption of 100% of the glucose and amino acids, 85% of the water that diffuses passively following an osmotic gradient, and 85% of the sodium chloride, which is transported by an active process involving the Na^+/K^+ -ATPase in the basolateral cell membranes. The proximal tubules also secrete into the lumen creatinine and foreign substances obtained from the interstitial plasma (Tisher and Brenner, 1994). Given these rigorous absorption and secretion activities, proximal tubular cells might be more susceptible to mildly defective focal adhesion complexes than to other regions of the kidney. Thus, even though tensin ablation does not prevent focal adhe-

sion assembly per se, it may weaken it in a fashion that could be responsive to fluid stresses. This notion is consistent with the reduction in focal adhesion immunolabeling in the cystic tubular cells (Fig. 9).

It is well documented from studies on cultured kidney epithelial cells that polarization is controlled not only by cell–substratum but also by cell–cell interactions (Wang et al., 1990*a*,*b*; for reviews see Drubin and Nelson, 1996; Eaton and Simons, 1995). While integrin-mediated cell–substratum interactions determine the orientation of the apicobasal axis (Wang et al., 1990*b*; Ojakian and Schwimmer, 1994), E-cadherin–mediated cell–cell contacts are required for basolateral formation (Vega-Salas et al., 1987; Gumbiner et al., 1988). In the future, it will be important to explore whether E-cadherin adherens junctions are perturbed in the cystic tubular cells of the tensin −/− kidneys. In addition, as we identify the specific domains of tensin that when missing are responsible for the defects we see in the kidneys, we should be able to assess whether the defects stem from loss of structural (i.e., actin-binding) activities, or alternatively from aberrancies in signal transduction. Finally, a key hypothesis as yet untested is the notion that structural deficiencies exist in the focal adhesions of tensin null proximal tubule cells, and that changes in focal adhesions precede the abnormalities seen in the tensin null kidneys. Sorting out the sequence of events between the loss of tensin and the development of abnormal kidney histology will be essential to our understanding of tensin's role in focal adhesion structure and function.

We especially thank Dr. Vikas Sukhatme and Dr. Mark Haas for their valuable discussions regarding the kidney defects observed in our knockout animals. Blood analysis was performed by the Animal Resource Center at the University of Chicago.

This work was supported by the Howard Hughes Medical Institutes (HHMI). S.H. Lo is a postdoctoral fellow of the HHMI; E. Fuchs is an investigator of the HHMI.

Received for publication 2 December 1996 and in revised form 17 January 1997.

References

Abercrombie, M., J. Heaysman, and S.M. Pegrum. 1971. The locomotion of fibroblasts in culture. *Exp. Cell Res.* 67:359–367.

Adra, C.N., P.H. Boer, and M.W. McBurney. 1987. Cloning and expression of the mouse pgk-1 gene and the nucleotide sequence of its promoter. *Gene (Amst.).* 60:65–74.

Auger, K.R., Z. Songyang, S.H. Lo, T.M. Boberts, and L.B. Chen. 1996. Platelet-derived growth factor-induced formation of tensin and phosphoinositide 3-kinase complexes. *J. Biol. Chem.* 271:23452–23457.

Bockholt, S.M., and K. Burridge. 1993. Cell spreading on extracellular matrix proteins induces tyrosine phosphorylation of tensin. *J. Biol. Chem.* 268:14565–14567.

Burridge, K., K. Fath, T. Kelly, G. Nuckolls, and C. Turner. 1988. Focal adhesions: transmembrane junctions between the extracellular matrix and the cytoskeleton. *Annu. Rev. Cell Biol.* 4:487–525.

Chiang, M.K., and J.G. Flanagan. 1996. PTP-NP, a new member of the receptor protein tyrosine phophatase family, implicated in development of nervous system and pancreatic endocrine cells. *Development (Camb.).* 122:2239–2250.

Chuang, J.Z., D.C. Lin, and S. Lin. 1995. Molecular cloning, expression, and mapping of the high affinity actin-capping domain of chicken cardiac tensin. *J. Cell Biol.* 128:1095–1109.

Davis, S., M.L. Lu, S.H. Lo, S. Lin, J.A. Butler, B.J. Druker, T.M. Roberts, Q. An, and L.B. Chen. 1991. Presence of an SH2 domain in the actin-binding protein tensin. *Science (Wash. DC).* 252:712–715.

Dowling, J., Q.C. Yu, and E. Fuchs. 1996. β4 integrin is required for hemidesmosome formation, cell adhesion and cell survival. *J. Cell Biol.* 134:559–572.

Drubin, D.G., and W.J. Nelson. 1996. Origins of cell polarity. *Cell.* 84:335–344.

Eaton, E., and K. Simons. 1995. Apical, basal, and lateral cues for epithelial polarization. *Cell.* 82:5–8.

Fassler, R., and M. Meyer. 1995. Consequences of lack of β1 integrin gene expression in mice. *Genes & Dev.* 9:1896–1908.

Furuta, Y., D. Ilic, S. Kanazawa, N. Takeda, T. Yamamoto, and S. Aizawa. 1995. Mesodermal defect in late phase of gastrulation by a targeted mutation of focal adhesion kinase, FAK. *Oncogene.* 11:1989–1995.

Georges-Labouesse, E., N. Messadeq, G. Yehia, L. Cadalbert, A. Dierich, and M. Le Meur. 1996. Absence of the α6 integrin leads to epidermolysis bullosa and neonatal death in mice. *Nat. Genet.* 13:370–373.

Glenney, J., and L. Zokas. 1989. Novel tyrosine kinase substrates from Rous sarcoma virus–transformed cells are present in the membrane skeleton. *J. Cell Biol.* 108:2401–2408.

Gumbiner, B., B. Stevenson, and A. Grimaldi. 1988. The role of the cell adhesion molecule uvomorulin in the formation and maintenance of the epithelial junctional complex. *J. Cell Biol.* 107:1575–1588.

Guo, L., L. Degenstein, J. Dowling, Q.C. Yu, R. Wollmann, B. Perman, and E. Fuchs. 1995. Gene targeting of BPAG1: abnormalities in mechanical strength and cell migration in stratified epithelia and neurologic degeneration. *Cell.* 81:233–244.

Horwitz, A., K. Duggan, C. Buck, M.C. Beckerle, and K. Burridge. 1986. Interactions of plasma membrane fibronectin receptor with talin—a transmembrane linkage. *Nature (Lond.).* 320:531–533.

Hynes, R.O. 1992. Integrins: versatility, modulation, and signaling in cell adhesion. *Cell.* 69:11–25.

Jockusch, B.M., P. Bubeck, K. Giehl, M. Kroemker, J. Moschner, M. Rothkegel, M. Rudiger, K. Schluter, G. Stanke, and J. Winkler. 1995. The molecular architecture of focal adhesions. *Annu. Rev. Cell Dev. Biol.* 11:379–416.

Junqueira, L.C., J. Carneiro, and R.O. Kelley. 1995. Basic Histology. Appleton and Lange, Stanford, CT. 488 pp.

Kanner, S.B., A.B. Reynolds, R.R. Vines, and J.T. Parsons. 1990. Monoclonal antibodies to individual tyrosine-phosphorylated protein substrates of oncogene-encoded tyrosine kinases. *Proc. Natl. Acad. Sci. USA.* 87:3328–3332.

Klein, G., M. Langegger, R. Timpl, and P. Ekblom. 1988. Role of laminin A chain in the development of epithelial cell polarity. *Cell.* 55:331–341.

Lo, S.H., Q. An, S. Bao, W. Wong, Y. Liu, P. Janmey, J.H. Hartwig, and L.B. Chen. 1994*a*. Molecular cloning of chick cardiac muscle tensin. *J. Biol. Chem.* 269:22310–22319.

Lo, S.H., P.A. Janmey, J.H. Hartwig, and L.B. Chen. 1994*b*. Interaction of tensin with actin and identification of its three distinct actin-binding domains. *J. Cell. Biol.* 125:1067–1075.

Lo, S.H., E. Weisberg, and L.B. Chen. 1994*c*. Tensin: a potential link between the cytoskeleton and signal transduction. *Bioessays.* 16:817–823.

Miyamoto, S., S.K. Akiyama, and K.M. Yamada. 1995. Synergistic roles for receptor occupancy and aggregation in integrin transmembrane function. *Science (Wash. DC).* 267:883–885.

Ojakian, G.K., and R. Schwimmer. 1994. Regulation of epithelial cell surface polarity reversal by β1 integrins. *J. Cell Sci.* 107:561–576.

Otey, C.A., F.M. Pavalko, and K. Burridge. 1990. An interaction between α-actinin and β1 integrin subunit in vitro. *J. Cell Biol.* 111:721–729.

Sakai, R., A. Iwamatsu, N. Hirano, S. Ogawa, T. Tanaka, H. Mano, Y. Yazaki, and H. Hirai. 1994. A novel signaling molecule, p130, forms stable complexes in vivo with v-Crk and v-Src in a tyrosine phosphorylation-dependent manner. *EMBO (Eur. Mol. Biol. Organ.) J.* 13:3748–3756.

Salgia, R., B. Brunkhorst, E. Pisick, J.L. Li, S.H. Lo, L.B. Chen, and J.D. Griffin. 1995. Increased tyrosine phosphorylation of focal adhesion proteins in myeloid cell lines expressing p210BCR/ABL. *Oncogene.* 11:1149–1155.

Schwartz, M.A., M.D. Schaller, and M.H. Ginsberg. 1995. Integrins: emerging paradigms of signal transduction. *Annu. Rev. Cell Dev. Biol.* 11:549–599.

Sorokin, L., A. Sonnenberg, M. Aumailley, R. Timpl, and P. Ekblom. 1990. Recognition of laminin E8 cell-binding site by an integrin possessing the α6 subunit is essential for epithelial polarization in developing kidney tubules. *J. Cell Biol.* 111:1265–1273.

Stephens, L., A. Sutherland, I. Klimanskaya, A. Andrieux, J. Meneses, R. Pedersen, and C. Damsky. 1995. Deletion of β1 integrins in mice results in inner cell mass failure and peri-implantation lethality. *Genes & Dev.* 9:1883–1895.

Tisher, C.C., and B.M. Brenner. 1994. Renal Pathology with Clinical and Functional Correlations. J.B. Lippincott Co., Philadelphia. 1694 pp.

Van der Neut, R., P. Krimpenfort, J. Calafat, C. Niessen, and A. Sonnenberg. 1996. Epithelial detachment due to absence of hemidesmosomes in integrin β4 null mice. *Nat. Genet.* 13:366–369.

Vega-Salas, D.E., P.J. Salas, D. Gundersen, and E. Rodriguez-Boulan. 1987. Formation of the apical pole of epithelial (Madin-Darby canine kidney) cells: polarity of an apical protein is independent of tight junctions while segregation of a basolateral marker requires cell–cell interactions. *J. Cell Biol.* 104:905–916.

Veis, D.J., C.M. Sorenson, J.R. Shutter, and S.J. Korsmeyer. 1993. Bcl-2-deficient mice demonstrate fulminant lymphoid apoptosis, polycystic kidneys, and hypopigmented hair. *Cell.* 75:229–240.

Wang, A.Z., G.K. Ojakian, and W.J. Nelson. 1990*a*. Steps in the morphogenesis of a polarized epithelium. I. Uncoupling the roles of cell-cell and cell-substratum contact in establishing plasma membrane polarity in multicellular epithelial (MDCK) cysts. *J. Cell Sci.* 95:137–151.

Wang, A.Z., G.K. Ojakian, and W.J. Nelson. 1990*b*. Steps in the morphogenesis of a polarized epithelium. II. Disassembly and assembly of plasma membrane domains during reversal of epithelial cell polarity in multicellular epithelial (MDCK) cysts. *J. Cell Sci.* 95:153–165.

Yu, Q.C., E. Allen, and E.V. Fuchs. 1996. Desmosomal disorganization and epidermal abnormalities in transgenic mouse expressing mutant desmoglein-3. *Proc. Microscopy Microanalysis.* 34–35.